Chemical Engineering Journal 416 (2021) 127662

Contents lists available at ScienceDirect

Chemical Engineering Journal

journal homepage: www.elsevier.com/locate/cej

Enhanced metal recovery by efficient agglomeration of precipitates in an up-flow fixed-bed bioreactor

Yun Liu [a,*], James Vaughan [b], Gordon Southam [c], Antonio Serrano [a], Esteban Marcellin [d], Ivan Nancucheo [e], Denys K. Villa-Gomez [a]

[a] School of Civil Engineering, The University of Queensland, 4072 QLD, Australia
[b] School of Chemical Engineering, The University of Queensland, 4072 QLD, Australia
[c] School of Earth and Environmental Sciences, The University of Queensland, 4072 QLD, Australia
[d] Australian Institute for Bioengineering and Nanotechnology, The University of Queensland, 4072 QLD, Australia
[e] Facultad de Ingeniería y Tecnología, Universidad San Sebastián, Lientur 1457, Concepción 4080871, Chile

ARTICLE INFO

Keywords:
Agglomeration
Extracellular polymeric substances (EPS)
Mine-impacted waters
Nickel
Cobalt
Sulfate reducing bacteria (SRB)

ABSTRACT

In this study, a single-stage up-flow fixed-bed sulfidogenic bioreactor was operated for 288 days (six stages), treating mine-impacted water at different concentrations of nickel (Ni), cobalt (Co) and other associated metals. The effect of metals on the sulfate reducing activity, metal recovery, extracellular proteins and microbial diversity was evaluated. The bioreactor configuration showed a positive synergistic effect on both sulfate reducing activity and metals recovery, which could treat up to 200 mg/L Ni. Over 99% of Ni and Co, as well as over 91% of the other metals in the influent, precipitated and settled in the bioreactor regardless of the initial metal concentration. The scanning electron microscopy (SEM) analysis of the precipitates showed the presence of extracellular polymeric substances (EPS), which may have helped to agglomerate the metal sulfide precipitates increasing their 'particle size' from 0.1 to 0.5 μm to 10–100 μm. Different extracellular proteins associated to these EPS increased in abundance upon variations of the bioreactor operation. These included proteins involved in enzymatic reactions and metal binding, such as periplasmic [NiFeSe] hydrogenase, standing out when Ni and Co was added. The biofilm characterization showed the dominance of metal-tolerant SRB genera (e.g., *Desulfomicrobium* spp. and *Desulfovibrio spp.*), but also of other non-SRB, demonstrating that a higher microbial diversity may help the biofilm endure higher metal concentrations.

1. Introduction

In recent years, the demand and price of metals with low natural abundance and unequal terrestrial distribution, classified as critical, have increased due to emerging technologies, such as smartphones, electric vehicles and green energy generation [1,2]. This is the case for nickel (Ni) and cobalt (Co), used in lithium-batteries of these technologies [3]. The demand for these metals has led to major economic, geopolitical, and environmental challenges [3,4] and to an increased interest for extracting these metals from secondary sources such as mine-impacted waters, i.e., tailings leachate, process wastewater, and acid mine drainage [5]. These mine-impacted waters contained significant amount of metals, which can cause toxicity to living organisms if not treated properly.

In the last decades, biological sulfate reduction process has been recognized as a technology for the treatment of mine-impacted waters that allows metal recovery [6]. In this process, sulfate-reducing bacteria (SRB) reduce sulfate to sulfide in the presence of electron donors, i.e., H_2 and CO_2/CO (autotrophs) or organic compounds (heterotrophs). The sulfide produced can precipitate metals, even at low metal concentrations and low pH as in mine-impacted waters [7]. The main advantage of the process for the mining industry is that it uses sulfate, another pollutant associated with these streams to produce sulfide on site, thus avoiding transportation of a hazardous chemical to remote areas.

In this process, due to the rapid precipitation of metal sulfides which favors nucleation over crystal growth, metal sulfide fines (particle size <0.5 μm) with poor settling properties tend to remain in the bulk effluent. This leads to low recovery efficiencies especially for Ni (43–85%), [8,9] as compared with other metals such as Cu and Zn (92–96%) [9,10]. Therefore, multiple-stage processes of separated

* Corresponding author.
E-mail address: y.liu4@uq.net.au (Y. Liu).

https://doi.org/10.1016/j.cej.2020.127662
Received 26 August 2020; Received in revised form 21 October 2020; Accepted 3 November 2020
Available online 9 November 2020

biological sulfate reduction and metal precipitation-flocculation-settling-filtration is the preferred option to recover metal precipitate fines; however, these measures increase the relevant costs due to additional reagents use/release and unit operations.

Over the last few years, there has been increasing interest in the use of simple, less expensive technologies [11], such as the application of simultaneous sulfate reduction and metal recovery in single-stage bioreactors [12,13]. This configuration possesses advantages in enhancing metal agglomeration and thus metal recovery by the bioreactor media components, i.e., volatile fatty acids (VFA), phosphate and extracellular polymeric substances (EPS) [8,14,15]. EPS are metabolic products that can bind to the cell surface or be released to the solution [16]. They mainly consist of proteins, polysaccharides, nucleic acids and other cellular components [17], and are typically reported to aid in the formation of a gel-like network that keeps bacteria together [18,19], influencing settling and dewaterability of sludge in wastewater treatment plants [20] and even metal removal [21]. The formation of EPS and their metal-binding ability is indeed affected by the hydraulic conditions [22] as well as the presence of metals [23]. However, the role of EPS on metal sulfide agglomeration, in particular the extracellular proteins, as main components in EPS, have been less studied. Better understanding on the interaction between metal sulfide and EPS/extracellular proteins is necessary to achieve efficient metal recovery.

In this study, mine-impacted water that contained significant amount of Ni (up to 200 mg/L) and other associated metals was treated in a single-stage up-flow fixed-bed bioreactor with recirculation. The objective was to assess how this configuration and metal loads affected the bacterial activity and how was this linked to metal recovery of the metal sulfide precipitates. For this, the microbial communities and their extracellular proteins were identified and quantified through metagenomic and proteomic analysis to better understand the conditions that can enhance EPS and thus agglomeration of metals. Furthermore, the development of the biofilm and the microbial diversity at different bioreactor periods were determined, thus providing insights for the extended application of the single-stage sulfidogenic bioreactor in the treatment of mine-impacted waters.

2. Materials and methods

2.1. Inoculum

The inoculum of the bioreactor was obtained from a lab-scale continuously stirred sulfidogenic bioreactor operated for over 300 days at hydraulic retention time (HRT) of 7 days, fed with lactate as substrate. A stepwise increase of Ni (0, 10, 50, 100 mg/L Ni) was added to the bioreactor to enrich Ni-tolerant SRB [27]. The sulfate reducing activity of the inoculum was 5.7 g sulfate/g volatile suspended solids (VSS) per day.

2.2. Bioreactor

An up-flow fixed-bed sulfidogenic bioreactor with a working volume of 1.4 L was used in this study (Fig. A1). Support material made of polyurethane foam (Merck, size = 10 × 10 cm, density = 0.08 g/cm^3, thickness = 1 cm) was cut into small pieces (2 cm^3), connected with polystyrene sticks, and fixed in the upper part of the bioreactor providing a surface for biofilm growth. The bioreactor had a recirculation pump that operated at 150 mL/min for complete mixing conditions [24]. After inoculation (0.021 g/L VSS), the bioreactor was operated for 288 days at 30C, a constant HRT of 2 days and a COD/sulfate ratio of 0.67.

A synthetic wastewater containing 2218 mg/L Na_2SO_4 as sulfate source (equivalent to 1500 mg/L sulfate), 1945 mg/L 60% sodium lactate as electron donor (equivalent to 1000 mg/L COD), and a mixture of macro- and micro-nutrients according to Zehnder et al. [25], was added to the bioreactor during the periods I to V. Once a steady state was achieved, i.e., the variations of effluent sulfide, sulfate and COD from last five HRT were lower than 10% [26], $NiCl_2$ was stepwise added in the influent (Table 1) from 100 mg/L Ni (period II) to 200 mg/L Ni (period III). As inhibition was observed in period III (Fig. 1), Ni concentration was decreased to 100 mg/L (period IV), after which both $NiCl_2$ and $CoCl_2$ (100 mg/L Ni and 10 mg/L Co, respectively) were added in the influent (period V). The pH of the synthetic metal-containing wastewater (periods II-V) was around 6.5. Finally, in period VI, the bioreactor was fed with diluted leachate (namely mine-impacted water) produced with tailings from the Old Tailings Dam, Savage River, Western Tasmania [29]. The leachate was diluted to match Ni and Co concentrations within the concentration range of a typical hydrometallurgical process [8]. Final metals composition and concentration in mg/L were: 100 Ni, 10 Co, 182 Al, 15 Cu and 8 Fe (Table 1). Other metal ions such as Mn, Zn, Pb and As were present at less than 2 mg/L with a pH of 3.3. The sulfate concentration in the diluted leachate was also adjusted from 341 mg/L to 1500 mg/L.

2.3. Sampling and analytical methods

Dissolved sulfide, sulfate and soluble COD and metals were measured by collecting effluent samples of the bioreactor after stopping recirculation for 5 min. Samples for metal measurements were taken only at the steady state of each period (i.e., period II to VI). At the end of each period, a small piece of the support material (0.02 cm^3) was cut off to characterize the biofilm through morphological and genomic analysis, while the precipitates from the reactor bottom were collected for morphological and mineralogical analysis.

A UV–VIS-NIR spectrophotometer (Shimadzu) was used to determine dissolved sulfide through the Cord-Ruwisch method [30], while ion chromatograph with conductivity (Thermo Scientific) was used to measure the sulfate concentration. Soluble COD was analyzed using Spectroquant® test kits and Prove 300 Photometer (Merck) after stripping H_2S with N_2 and filtering with 0.22 μm pore size filters. Total and soluble metal concentrations were measured with Inductive Coupled Plasma–Optical Emission Spectroscopy instrument (ICP-OES). For total metal measurements, samples were digested with 7% HNO_3 to dissolve all the metal precipitates present in the effluent. For soluble metal determination, samples were filtered (0.22 μm) first and then diluted in 7% HNO_3. Effluent pH was measured instantly by an online pH probe (E-514–2-000 S-can) coupled with D-313 S-can Terminal.

2.4. Calculations

Metal precipitation (Eq. (1)) in the bioreactor was defined as:

$$\text{Metal precipitation} = \frac{M_{in} - M_{out,soluble}}{M_{in}} \times 100\% \quad (1)$$

where M_{in} = metal concentration in the feed (mg/L); $M_{out,soluble}$ = soluble metal concentration (mg/L) in the effluent.

Metal settling (Equation (2)) in the bioreactor was defined as the amount of metal sulfide precipitates that settle in the bioreactor and thus were not drained in the effluent:

$$\text{Metal settling} = \frac{M_{in} - M_{out,total}}{M_{in}} \times 100\% \quad (2)$$

where $M_{out,total}$ = total metal concentration (mg/L) in the effluent.

The amount of metals accumulated in the bottom of the bioreactor during period IV were used to do the metal balance calculation of the metal recovery efficiency (Eq. (3)):

$$\text{Metal recovery} = \frac{M_t - M_b}{M_t} \times 100\% \quad (3)$$

where M_t = the amount of total metal (mg) in the influent that entered the bioreactor over period IV; M_b = the amount of metal (mg) from the

Table 1
Metal concentrations fed to the bioreactor at each period.

Synthetic wastewater									
Experimental period (days)	I (0–73)	II (74–136)	III (137–180)	IV (181–220)	V (221–257)				
Metal supplementation (mg/L)	—	Ni 100	Ni 200	Ni 100	Ni 100 + Co 10				
Mine-impacted water									
Experimental period (days)	VI (258–288)								
Metal supplementation (mg/L)	Al 182	Ni 100	Cu 15	Co 10	Fe 8	Mn 1.8	Zn 1	Pb 0.8	As 0.6

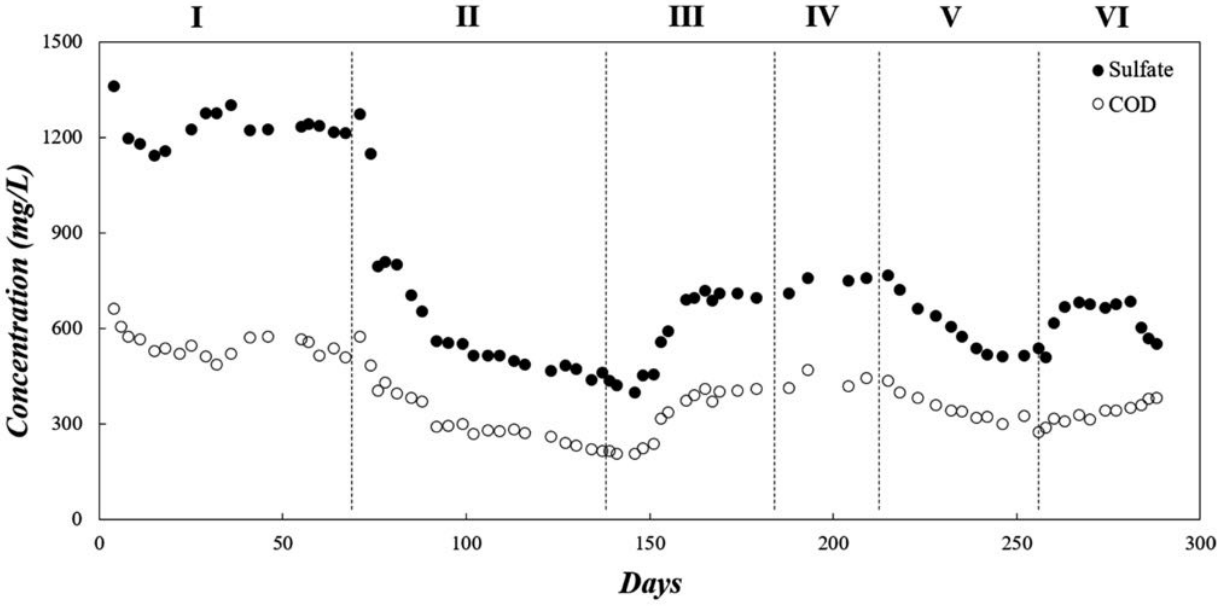

Fig. 1. Sulfate (●) and COD (○) concentration in the effluent during the operation of the up-flow fixed-bed sulfidogenic bioreactor.

bottom of the bioreactor over period IV.

Sulfate and COD removal (Eq. (4)) in the bioreactor were defined as:

$$R = \frac{C_{in} - C_{out}}{C_{out}} \times 100\% \quad (4)$$

where R is the sulfate or COD removal; C_{in} = sulfate or COD concentration in the feed (mg/L); C_{out} = sulfate or COD concentration (mg/L) in the effluent.

2.5. Characterization of the precipitates and biofilm

A Bruker D8 Advance powder X-ray diffractometer (XRD) with CuKα radiation was used to quantify the crystalline phases of the precipitates collected from the bottom of the bioreactor. The samples were prepared by washing with distilled water and drying at 40 °C. After grinding, the powder was loaded onto a sample holder and step-scanned from 10 to 80°2θ with a step size of 0.02°2θ and a counting time of 0.5°/min at 40 kV. The blank sample holder was also analyzed at the same condition as background. XRD pattern analysis was conducted with DIFFRAC.SUITE EVA software.

A JEOL JSM-7100F scanning electron microscope coupled with energy-dispersive X-ray spectroscopy (SEM-EDS) was used to characterize the precipitates collected from bioreactor bottom, as well as the biofilm growing on the support material. The biological samples were fixed with 2.5%$_{(aq)}$ glutaraldehyde for optimum preservation, then gradual dehydration was performed by immersing samples in 20, 40, 60, 80% and three times 100% ethanol [31]. Pelco Biowave Microwave was used to accelerate the dehydration process (40 s for each concentration of ethanol). The samples were then dried at the critical point in liquid CO_2 using Tousimis Autosamdri-815 CPD, after which they were mounted on stubs and coated with carbon using a Quorum Q150T coater. The Evactron 25 Plasma Cleaner was used to clean the carbon-coating samples before loading into the SEM. An accelerating voltage of 1 kV was applied for SEM imaging and 15 kV was applied for EDS analysis.

Ni precipitates were also prepared by using a sodium sulfide solution at 340 mg/L sulfide (similar as the concentration of the biogenic sulfide from the bioreactor) and 100 mg/L Ni and characterized using SEM for comparison with the precipitates collected from the bioreactor in this study (period II). The precipitates were filtered through Isopore^{TM} 0.1 μm filter papers, washed with distilled water then 100% ethanol, and air-dried for 24 h. The filter papers were loaded onto carbon tapes for carbon coating, plasma cleaning and SEM characterization as above mentioned.

2.6. Metagenomic and proteomic analysis

The metagenomic analysis of the biomass samples from each period of the bioreactor operation was carried out using the Illumina platform at the Australian Centre for Ecogenomics [32], which was then used as a data library for the proteomic analysis [28]. The Illumina reads were trimmed to 150 bases using TrimGalore (version 0.6.1; https://www.bioinformatics.babraham.ac.uk/projects/trim_galore/) and the quality was checked with FastQC (0.11.7; http://www.bioinformatics.babraham.ac.uk/projects/fastqc/). The trimmed reads were processed with Kraken2 (version 2.0.8-beta; https://doi.org/10.1186/s13059-019–1891-0) and Bracken 2.0.0 [33] to taxonomically classify the reads and determine the relative abundances of the RNA sequences as described in our previous research [28].

Proteins in the supernatant from each operational period of the bioreactor, namely extracellular proteins, were identified and quantified using a data-dependent acquisition (DDA) mass spectrometry (MS)

approach. The bioreactor effluent samples were firstly centrifuged at 2000×g for 5 min to obtain the supernatant. Then, an equal volume of 2X SDS protein solubilization buffer (10% SDS, 100 mM triethylammonium bicarbonate, TEAB, pH 7.55) was added to each supernatant sample. Alkylation of sulfhydryl groups and protein digestion was performed by adding dithiothreitol (DTT) to a final concentration of 20 mM and heated for 10 min at 95°C. Cysteines were alkylated by adding iodoacetamide to a final concentration of 100 mM and incubated for 30 min in the dark. Twelve percent aqueous phosphoric acid was added at 1:10 for a final concentration of 1.2% phosphoric acid; 3.3 mL of S-Trap buffer (90% aqueous methanol containing a final concentration of 100 mM TEAB, pH 7.1) was added to each sample and the mixture was loaded into S-traps. The S-trap was washed 3 times using S-Trap buffer. Proteins were digested on the filter for 16 h at 37°C with 1:50 trypsin/protein (V5073; Promega). Peptides were recovered by centrifuging the filters. Finally, the collected peptide material was dried in a vacuum centrifuge and mixed with 10 μL of 0.1% (v/v) formic acid (FA) in 5% (v/v) acetonitrile (ACN).

Liquid chromatography separation was performed using a Thermo-Scientific U3000 HPLC system, and the samples were then analyzed on the Q-Exactive HF (Thermo Fisher Scientific) in DDA mode as described by Valgepea, de Souza Pinto Lemgruber, Abdalla, Binos, Takemori, Takemori, Tanaka, Tappel, Köpke, Simpson, Nielsen and Marcellin [34]. Results from DDA analysis were used to build a spectral library and quantification was performed using Proteome Discoverer 2.4 (Thermo Fisher Scientific) against the database generated from the metagenomics analysis. Protein expression fold changes were determined using Proteome Discoverer 2.4.

3. Results

3.1. SRB activity in the bioreactor

After the steady state in period I, the sulfate reducing activity, measured as sulfate removal, varied with the changes in metal composition of the influent (Table 2 and Fig. 1). The highest sulfate removal efficiency was achieved at period II (69.1 ± 1.1%), when 100 mg/L Ni was fed to the bioreactor. When Ni increased to 200 mg/L at period III, sulfate removal decreased to 52.9 ± 0.5% (Table 2). Afterwards, Ni addition was adjusted back to 100 mg/L during period IV for biomass recovery; however, the sulfate removal efficiency remained at values similar to the previous period, indicating that the biomass conditions at period IV remained similar as the period III. Contrary, the co-addition of Ni and Co at period V increased the sulfate removal to 65.4 ± 0.7% (Table 2).

The feeding of mine-impacted water at period VI resulted in an initial slight decrease (Fig. 1) in sulfate reduction, probably due to the lower pH and higher metal concentrations (Table 2) in the influent. However, by day 278, the sulfate reducing activity recovered and thus, the sulfate removal was at the same range as the previous period (67.3 ± 2.8%). The effluent pH decreased from 6.7 to 6.0 ± 0.1 (Table 2) during the metal addition periods regardless of the higher acidity of the mine-impacted water.

The COD removal during the bioreactor operation showed a similar trend to sulfate reduction (Fig. 1), demonstrating that most of the COD was consumed by SRB (consumed COD/sulfate ratio of 0.63–0.74) except at period I, when COD removal (46.6 ± 2.5%) doubled the sulfate removal and the consumed COD/sulfate ratio was 1.76 (Table 2), indicating that other microorganisms apart from SRB were active at that period.

Table 2
Results of the bioreactor operation at the steady state of each period (mean ± standard deviation).

	Experimental periods					
	I	II	III	IV	V	VI
COD removal (%)	46.6 ± 2.5	77.4 ± 1.0	59.5 ± 0.4	57.3 ± 2.0	70.2 ± 1.8	63.2 ± 1.3
Sulfate removal (%)	17.6 ± 1.5	69.1 ± 1.1	52.9 ± 0.5	50.1 ± 1.3	65.4 ± 0.7	67.3 ± 2.8
Consumed COD/sulfate ratio	1.765	0.75	0.75	0.76	0.72	0.63
Effluent pH	6.6 ± 0.1	6.7 ± 0.1	6.4 ± 0.01	6.2 ± 0.1	6.0 ± 0.1	6.0 ± 0.1

3.2. Metal settling and recovery in the bioreactor

Over 99% of Ni and Co precipitated and settled in the bioreactor regardless of the metal addition period (Table 3), during which biologically produced sulfide to metal molar ratio was 6.3 (100 mg/L Ni), 2.4 (200 mg/L Ni), 4.6 (100 mg/L Ni), 5.4 (100 mg/L Ni + 10 mg/L Co), 1.2 (mine-impacted water), respectively. Despite the sufficient sulfide, Al and Fe in the mine-impacted water displayed lower precipitation (91–93%), but these precipitates were still effectively settled in the bioreactor as their settling values were almost equal to their precipitation rates. The Ni balance calculation showed that during period IV, the amount of Ni as precipitates that accumulated in the bottom of the bioreactor accounted for 80% of the total Ni fed during this period. The Ni precipitates that were neither in the effluent nor in the bioreactor bottom may have been accumulated on the biofilm (as backscattered SEM confirmed in Fig. A2), as well as biofilm support, bioreactor walls, or tubing.

3.3. Characterization of precipitates from the bioreactor bottom

The precipitates collected from the bioreactor were in the form of agglomerates and most of the size of the aggregates ranged between 10 and 100 μm (Fig. 2b), which are much larger than the 0.1–0.5 μm of particle size of Ni sulfides formed with chemical sulfide solution (Fig. 2a).

At high magnification, SEM-EDS analysis of the bioreactor precipitates denoted the presence of Ni sulfide minerals at a similar size as in the chemical sulfide solution, but entrapped with EPS along with microbial cells (Fig. 2c-e). The Ni sulfide crystalline phases were mainly heazlewoodite (Ni_3S_2) and polydymite (Ni_3S_4) (Fig. A3). The SEM images from period III at 200 mg/L Ni addition (Fig. 2d) displayed a greater amount of EPS and bacterial cells than the other metal addition periods. Interestingly, when the mine-impacted water was fed to the bioreactor, less EPS were observed in the precipitates (Fig. 2f).

Table 3
Metal precipitation and settling extents *(Italic in brackets)* during the bioreactor operation (mean ± standard deviation).

	Ni	Co	Al	Cu	Fe
II: 100 Ni	99.7 ± 0.1% *(99.2 ± 0.3%)*				
III: 200 Ni	99.8 ± 0.1% *(99.6 ± 0.1%)*				
IV: 100 Ni	99.6 ± 0.0% *(99.2 ± 0.3%)*				
V: 100 Ni + 10 Co	99.9 ± 0.0% *(99.3 ± 0.2%)*	99.8 ± 0.0% *(99.4 ± 0.1%)*			
VI: mine-impacted water	99.9 ± 0.0% *(99.8 ± 0.1%)*	99.9 ± 0.0% *(99.7 ± 0.2%)*	91.4 ± 0.0% *(91.4 ± 0.1%)*	99.8 ± 0.1% *(99.6 ± 0.3%)*	93.3 ± 0.0% *(92.9 ± 0.1%)*

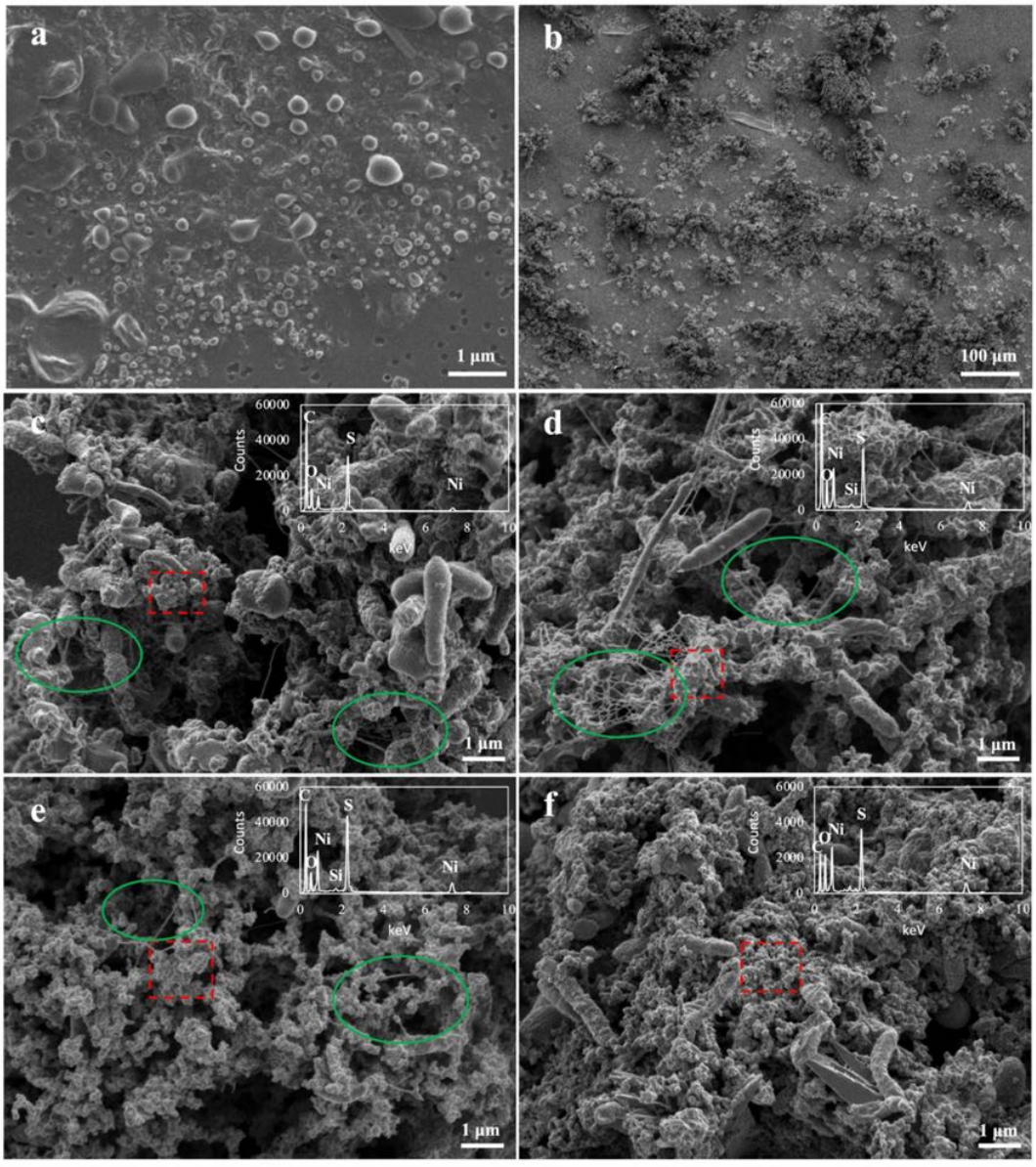

Fig. 2. Secondary electron scanning electron micrographs of filtered Ni sulfide precipitates collected from (a) chemical sulfide solution, and the bioreactor bottom at (b-c) period II (100 mg/L Ni); (d) period III (200 mg/L Ni); (e) period V (100 mg/L Ni and 10 mg/L Co); and (f) period VI (mine-impacted water). Note the presence of Ni sulfide grains (red rectangle) and 'filaments' of dehydrated extracellular polymeric substances (green circle). EDS data on the upright corner of each graph showed that the main components of these precipitates were Ni sulfides. (For interpretation of the references to color in this figure legend, the reader is referred to the web version of this article.)

3.4. Extracellular protein characterization

A total of 559 protein groups were identified and 49 proteins were found differentially expressed across any comparison among all the periods (Fig. 3). The functions of the identified proteins were also collected, although some functions were marked as unknown as the current protein databases are still limited.

With the addition of 100 mg/L Ni in period II, three proteins were found having higher abundance than in the other periods, i.e., ATP synthase subunit alpha, sulfate adenylyltransferase (*Desulfatibacillum*) and toxin RTX-I translocation ATP-binding protein. The function of sulfate adenylyltransferase is related to ATP binding, hydrogen sulfide biosynthetic and sulfate assimilation process (Table A1), corresponding to the highest sulfate reducing activity at this period (Table 2). When Ni concentration increased to 200 mg/L in period III, the abundance of the previously mentioned proteins decreased along with the sulfate reducing activity (Table 2) and shifted the abundance to a different subgroup of fifteen proteins, possessing a range of enzymatic reactions, e.g., a branched-chain-amino-acid aminotransferase, and a serine hydroxymethyltransferase (Table A1). In this period, there were also proteins capable of binding and transporting amino acids, ATP or metal ions (Table A1), such as tungstate-binding protein, porin D, solute-binding protein and type II secretion system protein E. When both Ni and Co were added to the bioreactor in period V, proteins including periplasmic [NiFeSe] hydrogenase large subunit, sulfate adenylyltransferase (*Desulfovibrio*) and adenylylsulfate reductase subunit alpha showed the highest abundance among all the experimental periods. During the last period, fed with mine-impacted water, the abundance of the proteins expressed in Ni-Co period decreased, while other proteins increased in abundance, i.e., 60 kDa chaperonin, tRNA-specific 2-thiouridylase MnmA and rubredoxin-oxygen oxidoreductase (Fig. 3).

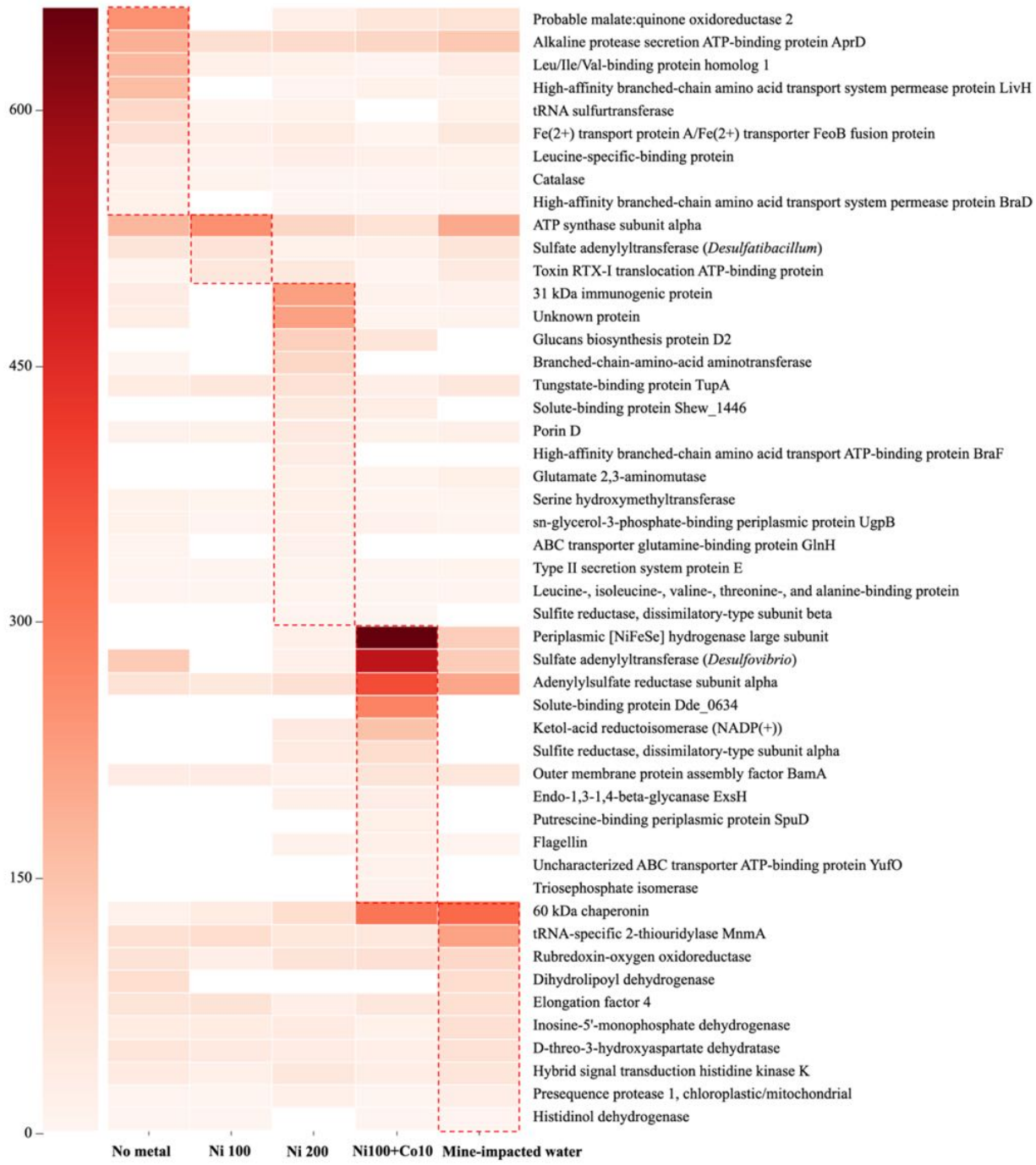

Fig. 3. Heatmap of extracellular proteins in each period of the bioreactor operation. The color intensity is related to the relative abundance, ranging from white (low abundance) to dark red (high abundance). Note that the proteins within the red rectangle have the highest abundance among all the experimental periods. (For interpretation of the references to color in this figure legend, the reader is referred to the web version of this article.)

3.5. Bacterial population growth in the biofilm

The morphological variation of the support material and biofilms before and after the addition of metals to the bioreactor are shown in Fig. 4. At first, the surface of the support material was relatively clean. After approximately two months of bioreactor operation without metal supplementation, rod-like bacteria adhered on the support material. During the subsequent periods, under different metal amendments, SRB colonized and formed a thicker biofilm comprised of a more structurally diverse consortium of microbial species filling the porosity of the support material.

The addition of metals to the bioreactor affected the microbial diversity. During the period I, i.e., without metal addition, the dominant species were affiliated with members of the genera *Desulfomicrobium, Pseudomonas, Wolinella,* and *Stenotrophomonas* (Fig. 5). With the addition of 100 mg/L Ni at period II, the various *Pseudomonas* species were inhibited, while species belonging to the genera *Desulfomicrobium, Desulfovibrio, Proteiniphilum, Ralstonia, Delftia* increased (Fig. 5), suggesting that these species are more Ni-resistant. However, when Ni concentration increased to 200 mg/L at period III, the relative abundance of almost all the species decreased, with *Desulfomicrobium baculatum, Wolinella succinogenes* and *Pseudomonas fluorescens* more dominant than other species (Fig. 5). After a period of recovery at the lower Ni concentration (100 mg/L), Co was supplemented to the

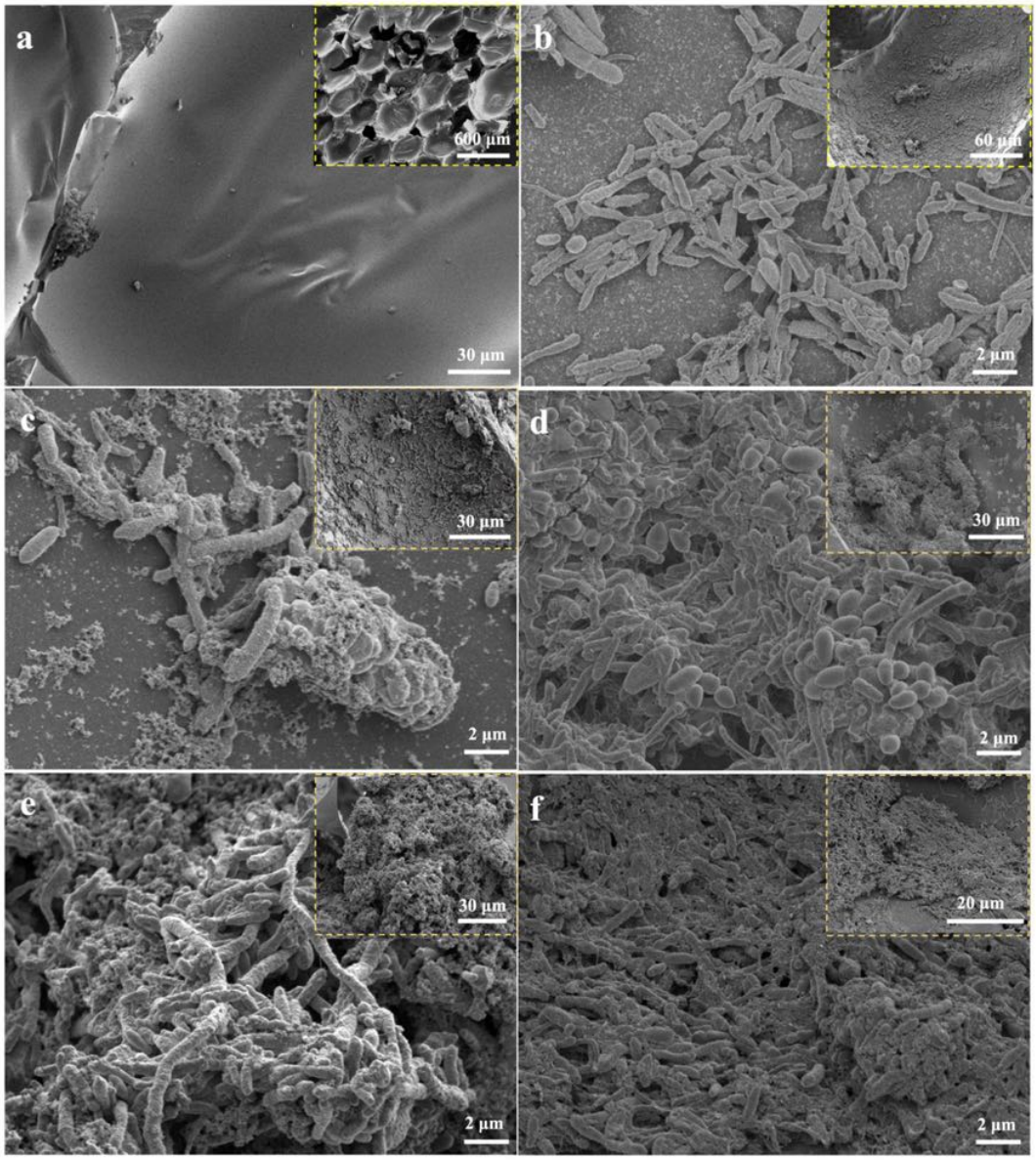

Fig. 4. Secondary electron scanning electron micrographs of (a) the original support material, and biofilms attached on the support material collected from the bioreactor operated at: (b) no metal addition; (c) 100 mg/L Ni; (d) 200 mg/L Ni; (e) 100 mg/L Ni and 10 mg/L Co; (f) mine-impacted water.

bioreactor (period V) and the previous species abundance recovered where species such as *Desulfovibrio alaskensis* and *Stenotrophomonas maltophilia* were even more abundant than when solely fed 100 mg/L Ni (Fig. 5). During the last period when the mine-impacted water containing multiple metals and lower pH was fed to the bioreactor, the dominant species remained similar to the previous Ni-Co period (Fig. 5).

4. Discussion

4.1. Effect of agglomeration on Ni recovery

This study demonstrated that the Ni sulfide precipitates in a one-stage bioreactor agglomerated, producing a particle size range from 10 to 100 µm. This resulted in better settling properties with less than 1% of these precipitates washed out in the effluent regardless of the influent metal concentrations (Table 3). This is in contrast with previously reported values in fluidized-bed bioreactors, with 14 to 50% of the metals draining off as metal precipitates [13,35]. Remarkably, the individual precipitates collected from the bioreactor bottom were composed of numerous 0.1–0.5 µm Ni sulfide crystals (Fig. 2, red rectangle) including heazlewoodite and polydymite (Fig. A3) [36,37]. These Ni sulfide precipitates had a similar size as the precipitates formed with chemical sulfide (Fig. 2a), indicating that the particle growth of these precipitates from bioreactor was mainly attributed to agglomeration rather than crystal growth, as reported in previous studies in bioreactors [38,39].

In this study, it was observed that the agglomeration of metal sulfides was linked with the generation of EPS (Fig. 2, green circle), which can act as a flocculant [40], trapping the small, sub-µm-scale metal sulfide crystals. The EPS possesses both positive and negative functional groups so that the charge neutralization mechanism could make these precipitates interact and form larger agglomerates [17,41,42]. The high Ni concentration may enhance the production and activity of the EPS, which can help to protect microbes from the harsh environment [15]. Accordingly, a stronger presence of EPS was observed at 200 mg/L Ni (Fig. 2d).

Apart from EPS, other compounds such as phosphate, acetate and sulfate that are most commonly found in a sulfidogenic bioreactor could

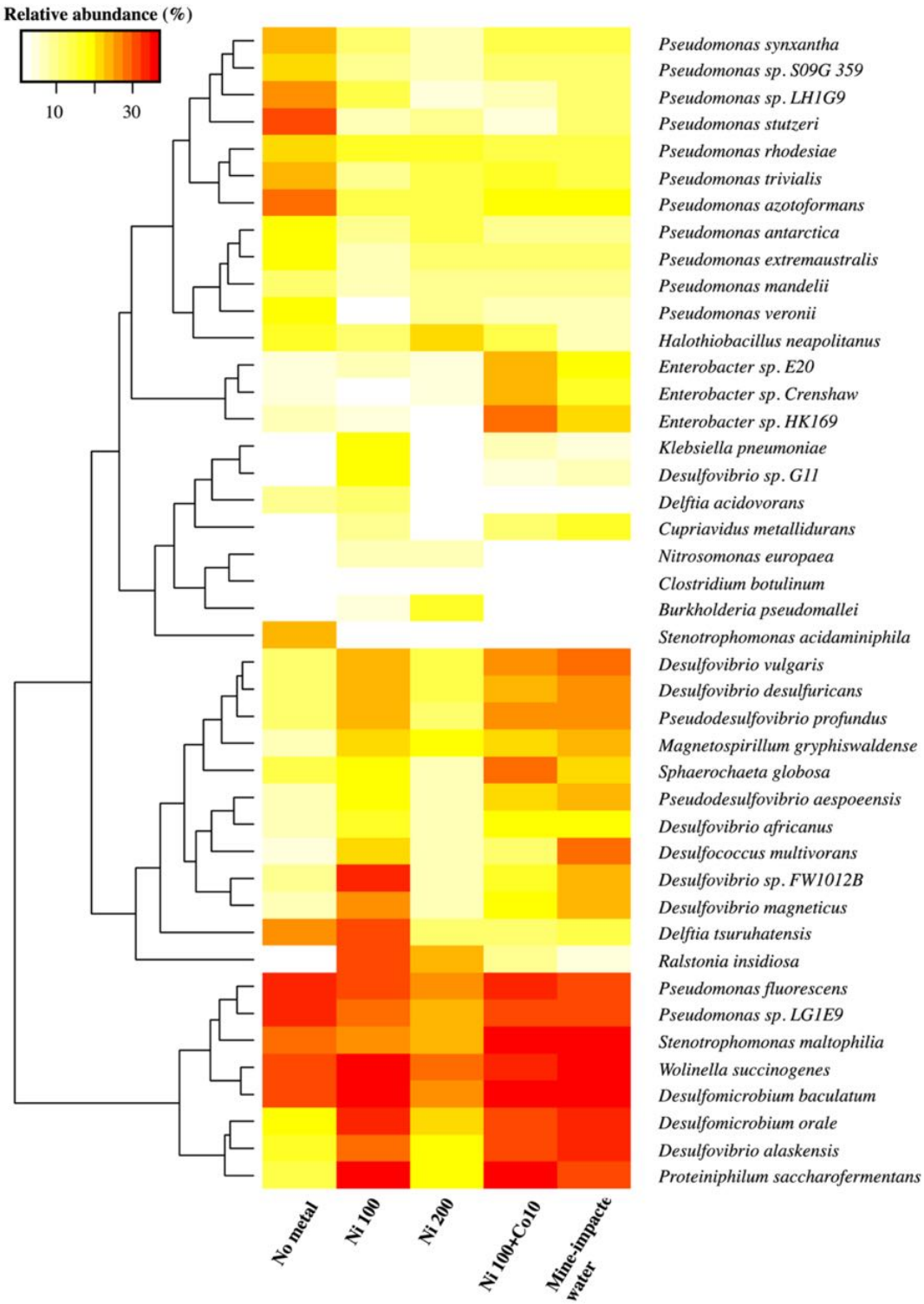

Fig. 5. Heatmap of the relative abundance and distribution of the RNA sequences in each period of the bioreactor operation. The color intensity is related to the relative abundance, ranging from white (low abundance) to yellow to red (high abundance). (For interpretation of the references to color in this figure legend, the reader is referred to the web version of this article.)

also enhance agglomeration of the precipitates [8]. In our previous study, assessing Ni precipitation with sulfide, bigger aggregates were formed with biogenic sulfide (8.1 ± 0.3 μm) as compared to the ones formed with chemical sulfide (1.0 ± 0.1 μm) due to the presence of the above-mentioned compounds in the biogenic sulfide. However, these particle sizes are still smaller than the precipitates formed in this study (10–100 μm). The increase in particle size may also be due to the presence of EPS as well as the hydrodynamic conditions in the bioreactor, which are known to enhance contact due to the mixing conditions [24,43] and aggregation of the precipitates due to seeding [44].

4.2. Effect of metal addition on SRB activity

This study showed that both the sulfate reducing activity and metal

recovery in the proposed bioreactor can successfully treat mine-impacted water containing 100–200 mg/L Ni, much higher than previously reported (25 mg/L Ni) causing reduced sulfate reducing activity [45]. The operation of the sulfidogenic bioreactor shows that the presence of metals could create a positive synergistic effect on sulfate reducing activity and Ni precipitation, resulting in an increased sulfate removal from 17.6 ± 1.5% up to a maximum of 69.1 ± 1.1% with the addition of 100 mg/L Ni (Table 2). This could be attributed to the EPS that accumulated outside the cells could protect the SRB (*Desulfomicrobium* and *Desulfovibrio*; Fig. 5) from metal toxicity through complexation or adsorption [46]. Then the sulfide produced by the SRB would precipitate the metals, resulting in the reduced toxicity of free Ni as well as removing the inhibitory effect of sulfide ions to SRB [31]. In agreement with our previous study [28], Co addition in period V, as well as the addition of other metals when mine-impacted water was fed, enhanced the biological sulfate reduction (Table 2). This is explained by the role of Co and other metals as essential nutrient enhancing the microbial activity [47].

The lowest sulfate removal was observed in period III at 200 mg/L Ni addition (52.9 ± 0.5%), which pointed to inhibition to SRB, as threshold values reported were surpassed [48]. Despite this, the sulfate reducing activity obtained in this period (397 mg/(L·d)), was still higher as compared to the best value reported in inversed fluidized bed bioreactors at lower Ni concentrations [45].

4.3. Effect of metal addition on proteins production

High-throughput proteomic analysis was used to identify and quantify the extracellular proteins at each experimental period to understand the conditions that can enhance EPS production, as they contributed to metal sulfide agglomeration (Fig. 2, green circle). The identified proteins and functions helped to enrich our understanding of the process occurring in sulfate reducing bioreactors treating Ni-containing mine impacted waters.

Results showed that the diversity and quantity of extracellular proteins markedly varied depending on the type and concentration of metals in each bioreactor period (Fig. 3), which is in agreement with previous research showing that microbial responses generating extracellular proteins is dependent to these [15,28,49].

When Ni concentration increased to 200 mg/L, all the protein abundance of previous periods decreased, in agreement with the decrease of the sulfate reducing activity due to Ni inhibition (Table 2). Nevertheless, other proteins showed abundance (Table A1), which corresponds to the stronger presence of EPS observed at this period that contributed to flocculation, settling and dewatering [15].

Period V, where both Ni and Co were added, displayed the higher concentration of proteins among all bioreactor operation, with the highest abundance of periplasmic [NiFeSe] hydrogenase (Fig. 3). Hydrogenases can catalyze the oxidation and utilization of molecular hydrogen, which was intimately involved in the metabolism of SRB [50]. Previous studies have shown that this protein has Ni binding ability through bridging cysteine thiolates [51], which might have contributed to the reduced Ni toxicity to SRB and the increased sulfate reducing activity at this period.

4.4. Effect of metal addition on biofilm community

The complex biofilm formed in the sulfidogenic bioreactor and the dominant metal-tolerant genera (e.g., *Desulfomicrobium* and *Desulfovibrio*) allowed the single-stage bioreactor to endure toxic concentrations of metals, thus improving the robustness of the bioreactor. The dense biofilm was formed on the fixed bed (Fig. 4) enhance by the recirculation in the bioreactor, which provided high hydraulic shear force on the support materials to minimize the accumulation of excessive metal precipitates on the biofilm [24]. The dominant sulfate reducing genera detected in the biofilm throughout most of the bioreactor operation were mainly affiliated with *Desulfomicrobium* and *Desulfovibrio* (Fig. 5), confirming the metals resistance capability of these genera [52,53]. Apart from the SRB, the occurrence of other non-sulfate-reducing microbes such as *Wolinella, Proteiniphilum*, *Ralstonia, Pseudomonas* and *Delftia* were also identified when Ni, Co and other metals were supplemented (Fig. 5), indicating that these microbes could also have metal resistance ability. Moreover, the co-existence of both SRB and non-SRB demonstrated that a higher microbial diversity may help the biofilm endure higher metal concentrations [54]. The cooperation of these microbial species may allow getting over metal toxicity by impeding metal cation access to the biofilm or into the cells [6,55,56]. Therefore, the application of complex consortia possessing metal-tolerant species can be beneficial to directly treat mine-impacted water, since the increased microbial diversity could help stabilize the biofilm's function under fluctuating conditions [57].

5. Conclusions

- The proposed single-stage up-flow fixed-bed sulfidogenic bioreactor showed a positive synergistic effect on sulfate reducing activity and Ni recovery, which could endure as high as 200 mg/L Ni.
- Over 99% of Ni and Co precipitated and settled in the bioreactor due to the efficient agglomeration, which is enhanced by the high recirculation rate and the EPS generated due to Ni stress.
- Ni, Co and a range of metals from the mine-impacted water resulted in the variation in the generation of extracellular proteins, which is also connected to the variation in sulfate reducing activity.
- The genera *Desulfomicrobium* and *Desulfovibrio* were mainly responsible for the high sulfate reducing activity under Ni stress.

Declaration of Competing Interest

The authors declare that they have no known competing financial interests or personal relationships that could have appeared to influence the work reported in this paper.

Acknowledgement

This research work was funded by the University of Queensland through to the project UQECR1946429. The authors would like to thank Dr. Robin Palfreyman for helping with metagenomic analysis and Dr. Gert Talbo for LCMS analysis and sample preparation. The authors thank the laboratory staff of the Australian Microscopy & Microanalysis Research Facility and Advanced Water Management Centre at UQ for the analytical support and to Anita Parbhakar-Fox and collaborators for providing the mine-impacted water used in this study. The proteomics analysis was performed by the Queensland Node of Metabolomics Australia, an NCRIS funded initiative funded through Bioplatforms Australia (BPA).

Appendix A. Supplementary data

Supplementary data to this article can be found online at https://doi.org/10.1016/j.cej.2020.127662.

References

[1] T. Hennebel, N. Boon, S. Maes, M. Lenz, Biotechnologies for critical raw material recovery from primary and secondary sources: R&D priorities and future perspectives, New Biotechnol. 32 (2015) 121–127.
[2] W.Q. Zhuang, J.P. Fitts, C.M. Ajo-Franklin, S. Maes, L. Alvarez-Cohen, T. Hennebel, Recovery of critical metals using biometallurgy, Curr. Opin. Biotechnol. 33 (2015) 327–335.
[3] P. Meshram, B.D. Abhilash, Pandey, Advanced review on extraction of nickel from primary and secondary sources, Miner. Process. Extr. Metall. Rev. 40 (2018) 157–193.

[4] X. Fu, D.N. Beatty, G.G. Gaustad, G. Ceder, R. Roth, R.E. Kirchain, M. Bustamante, C. Babbitt, E.A. Olivetti, Perspectives on cobalt supply through 2030 in the face of changing demand, Environ. Sci. Technol. 54 (2020) 2985–2993.

[5] Y. Liu, A. Serrano, D. Villa-Gomez, Biological treatment of mine-impacted waters on the context of metal recovery. in: The Future of Effluent Treatment Plants-Biological Treatment Systems, (Eds.) M.P. Shah, S.R. Couto, K. Mehta, India, Elsevier, 2021, DOI: 10.1016/C2019-0-04851-0 (in print).

[6] M. Gopi Kiran, K. Pakshirajan, G. Das, An overview of sulfidogenic biological reactors for the simultaneous treatment of sulfate and heavy metal rich wastewater, Chem. Eng. Sci. 158 (2017) 606–620.

[7] A.E. Lewis, Review of metal sulphide precipitation, Hydrometallurgy 104 (2010) 222–234.

[8] Y. Liu, A. Serrano, J. Vaughan, G. Southam, L. Zhao, D. Villa-Gomez, The influence of biologically produced sulfide-containing solutions on nickel and cobalt precipitation reactions and particle settling properties, Hydrometallurgy 189 (2019), 105142.

[9] A.H. Kaksonen, L. Lavonen, M. Kuusenaho, A. Kolli, H. Närhi, E. Vestola, J. A. Puhakka, O.H. Tuovinen, Bioleaching and recovery of metals from final slag waste of the copper smelting industry, Miner. Eng. 24 (2011) 1113–1121.

[10] E. Sahinkaya, M. Gungor, Comparison of sulfidogenic up-flow and down-flow fluidized-bed reactors for the biotreatment of acidic metal-containing wastewater, Bioresour. Technol. 101 (2010) 9508–9514.

[11] K. Brahmi, W. Bouguerra, S. Harbi, E. Elaloui, M. Loungou, B. Hamrouni, Treatment of heavy metal polluted industrial wastewater by a new water treatment process: Ballasted electroflocculation, J. Hazard. Mater. 344 (2018) 968–980.

[12] E. Sahinkaya, A. Yurtsever, E. Isler, I. Coban, O. Aktas, Sulfate reduction and filtration performances of an anaerobic membrane bioreactor (AnMBR), Chem. Eng. J. 349 (2018) 47–55.

[13] D. Villa-Gomez, H. Ababneh, S. Papirio, D.P. Rousseau, P.N. Lens, Effect of sulfide concentration on the location of the metal precipitates in inversed fluidized bed reactors, J. Hazard. Mater. 192 (2011) 200–207.

[14] D. Villa-Gomez, E.D. van Hullebusch, R. Maestro, F. Farges, S. Nikitenko, H. Kramer, G. Gonzalez-Gil, P.N.L. Lens, Morphology, mineralogy, and solid-liquid phase separation characteristics of Cu and Zn precipitates produced with biogenic sulfide, Environ. Sci. Technol. 48 (2014) 664–673.

[15] T.T. More, J.S. Yadav, S. Yan, R.D. Tyagi, R.Y. Surampalli, Extracellular polymeric substances of bacteria and their potential environmental applications, J. Environ. Manage. 144 (2014) 1–25.

[16] X. Zhou, Z. Chen, Z. Li, H. Wu, Impacts of aeration and biochar addition on extracellular polymeric substances and microbial communities in constructed wetlands for low C/N wastewater treatment: Implications for clogging, Chem. Eng. J. 396 (2020), 125349.

[17] W.W. Li, H.Q. Yu, Insight into the roles of microbial extracellular polymer substances in metal biosorption, Bioresour. Technol. 160 (2014) 15–23.

[18] P. d'Abzac, F. Bordas, E. Joussein, E. van Hullebusch, P.N.L. Lens, G. Guibaud, Characterization of the mineral fraction associated to extracellular polymeric substances (EPS) in anaerobic granular sludges, Environ. Sci. Technol. 44 (2010) 412–418.

[19] Y. Shi, J. Huang, G. Zeng, Y. Gu, Y. Chen, Y. Hu, B. Tang, J. Zhou, Y. Yang, L. Shi, Exploiting extracellular polymeric substances (EPS) controlling strategies for performance enhancement of biological wastewater treatments: An overview, Chemosphere 180 (2017) 396–411.

[20] J.I. Houghton, T. Stephenson, Effect of influent organic content on digested sludge extracellular polymer content and dewaterability, Water Res. 36 (2002) 3620–3628.

[21] G. Guibaud, E. van Hullebusch, F. Bordas, P. d'Abzac, E. Joussein, Sorption of Cd (II) and Pb(II) by exopolymeric substances (EPS) extracted from activated sludges and pure bacterial strains: Modeling of the metal/ligand ratio effect and role of the mineral fraction, Bioresour. Technol. 100 (2009) 2959–2968.

[22] M.L. Sesay, G. Özcengiz, F. Dilek Sanin, Enzymatic extraction of activated sludge extracellular polymers and implications on bioflocculation, Water Res. 40 (2006) 1359–1366.

[23] Z.-B. Yue, Q. Li, C.-C. Li, T.-H. Chen, J. Wang, Component analysis and heavy metal adsorption ability of extracellular polymeric substances (EPS) from sulfate reducing bacteria, Bioresour. Technol. 194 (2015) 399–402.

[24] J. Chung, R. Nerenberg, B.E. Rittmann, Bioreduction of selenate using a hydrogen-based membrane biofilm reactor, Environ. Sci. Technol. 40 (2006) 1664–1671.

[25] A.J.B. Zehnder, B.A. Huser, T.D. Brock, K. Wuhrmann, Characterization of an acetate-decarboxylating, non-hydrogen-oxidizing methane bacterium, Arch. Microbiol. 124 (1980) 1–11.

[26] A. Bayrakdar, E. Sahinkaya, M. Gungor, S. Uyanik, A.D. Atasoy, Performance of sulfidogenic anaerobic baffled reactor (ABR) treating acidic and zinc-containing wastewater, Bioresour. Technol. 100 (2009) 4354–4360.

[27] Y. Liu, A. Serrano, V. Wyman, G. Southam, J. Vaughan D. Villa-Gomez, Ni stress to sulphate reducing bacteria enhances Ni complexation: Opportunity for Ni-Co separation from wastewater, in: 16th World Congress on Anaerobic Digestion. Delft, The Netherlands, 2019.

[28] Y. Liu, A. Serrano, V. Wyman, E. Marcellin, G. Southam, J. Vaughan, D. Villa-Gomez, Nickel complexation as an innovative approach for nickel-cobalt selective recovery using sulfate-reducing bacteria, J. Hazard. Mater. 402 (2021), 123506.

[29] A. Parbhakar-Fox, J. Glen, B. Raimondo, A geometallurgical approach to tailings management: An example from the Savage River Fe-ore mine, Western Tasmania, Minerals 8 (2018) 454.

[30] R. Cord-Ruwisch, A quick method for the determination of dissolved and precipitated sulfides in cultures of sulfate-reducing bacteria, J. Microbiol. Methods 4 (1985) 33–36.

[31] D. González, Y. Liu, D. Villa Gomez, G. Southam, S. Hedrich, P. Galleguillos, C. Colipai, I. Nancucheo, Performance of a sulfidogenic bioreactor inoculated with indigenous acidic communities for treating an extremely acidic mine water, Miner. Eng. 131 (2019) 370–375.

[32] G. Kong, S. Ellul, V. Narayana, K. Kanojia, H.T.T. Ha, S. Li, T. Renoir, K.-A.L. Cao, A. Hannan, An integrated metagenomics and metabolomics approach implicates the microbiome-gut-brain-axis in the pathogenesis of Huntington's disease transgenic mice, PREPRINT (Version 1) available at Research Square [+https://doi.org/10.21203/rs.2.23316/v1+] (2020).

[33] J. Lu, F.P. Breitwieser, P. Thielen, S.L. Salzberg, Bracken: Estimating species abundance in metagenomics data, PeerJ Comput. Sci. 3 (2017), e104.

[34] K. Valgepea, R. de Souza Pinto, T. Lemgruber, S. Abdalla, N. Binos, A. Takemori, Y. Takemori, R. Tanaka, M. Tappel, S.D. Köpke, L.K. Simpson, E.M. Nielsen, H_2 drives metabolic rearrangements in gas-fermenting *Clostridium autoethanogenum*, Biotechnol. Biofuels 11 (2018) 55.

[35] A.H. Kaksonen, M.L. Riekkola-Vanhanen, J.A. Puhakka, Optimization of metal sulphide precipitation in fluidized-bed treatment of acidic wastewater, Water Res. 37 (2003) 255–266.

[36] J.P. Gramp, J.M. Bigham, K. Sasaki, O.H. Tuovinen, Formation of Ni- and Zn-sulfides in cultures of sulfate-reducing bacteria, Geomicrobiol J. 24 (2007) 609–614.

[37] P. Kousi, E. Remoundaki, A. Hatzikioseyian, F. Battaglia-Brunet, C. Joulian, V. Kousteni, M. Tsezos, Metal precipitation in an ethanol-fed, fixed-bed sulphate-reducing bioreactor, J. Hazard. Mater. 189 (2011) 677–684.

[38] D.K. Villa-Gomez, S. Papirio, E.D. van Hullebusch, F. Farges, S. Nikitenko, H. Kramer, P.N.L. Lens, Influence of sulfide concentration and macronutrients on the characteristics of metal precipitates relevant to metal recovery in bioreactors, Bioresour. Technol. 110 (2012) 26–34.

[39] F.D. Reis, A.M. Silva, E.C. Cunha, V.A. Leão, Application of sodium- and biogenic sulfide to the precipitation of nickel in a continuous reactor, Sep. Purif. Technol. 120 (2013) 346–353.

[40] M. Shahadat, T.T. Teng, M. Rafatullah, Z.A. Shaikh, T.R. Sreekrishnan, S.W. Ali, Bacterial bioflocculants: A review of recent advances and perspectives, Chem. Eng. J. 328 (2017) 1139–1152.

[41] Y. Liu, S.Q. Li, S.M. Luo, W. Wei, Speciation characterization of efficient composite inorganic polymer flocculant-poly-ferric-zinc-silicate-sulphate, Asian J. Chem. 26 (2014) 5677–5681.

[42] P. d'Abzac, F. Bordas, E. Joussein, E.D. van Hullebusch, P.N.L. Lens, G. Guibaud, Metal binding properties of extracellular polymeric substances extracted from anaerobic granular sludges, Environ. Sci. Pollut. Res. 20 (2013) 4509–4519.

[43] E. Sahinkaya, F.M. Gunes, D. Ucar, A.H. Kaksonen, Sulfidogenic fluidized bed treatment of real acid mine drainage water, Bioresour. Technol. 102 (2011) 683–689.

[44] D. Guillard, A.E. Lewis, Nickel carbonate precipitation in a fluidized-bed reactor, Ind. Eng. Chem. Res. 40 (2001) 5564–5569.

[45] S. Janyasuthiwong, E.R. Rene, G. Esposito, P.N.L. Lens, Effect of pH on Cu, Ni and Zn removal by biogenic sulfide precipitation in an inversed fluidized bed bioreactor, Hydrometallurgy 158 (2015) 94–100.

[46] Z. Teng, W. Shao, K. Zhang, Y. Huo, J. Zhu, M. Li, Pb biosorption by *Leclercia adecarboxylata*: Protective and immobilized mechanisms of extracellular polymeric substances, Chem. Eng. J. 375 (2019), 122113.

[47] J.B. Glass, S. Chen, K.S. Dawson, D.R. Horton, S. Vogt, E.D. Ingall, B.S. Twining, V. J. Orphan, Trace metal imaging of sulfate-reducing bacteria and methanogenic archaea at single-cell resolution by synchrotron X-ray fluorescence imaging, Geomicrobiol J. 35 (2018) 81–89.

[48] J. Gustavsson, S. Shakeri Yekta, C. Sundberg, A. Karlsson, J. Ejlertsson, U. Skyllberg, B.H. Svensson, Bioavailability of cobalt and nickel during anaerobic digestion of sulfur-rich stillage for biogas formation, Appl. Energy 112 (2013) 473–477.

[49] J. Wang, Q. Li, M.-M. Li, T.-H. Chen, Y.-F. Zhou, Z.-B. Yue, Competitive adsorption of heavy metal by extracellular polymeric substances (EPS) extracted from sulfate reducing bacteria, Bioresour. Technol. 163 (2014) 374–376.

[50] S.M. Caffrey, H.-S. Park, J.K. Voordouw, Z. He, J. Zhou, G. Voordouw, Function of periplasmic hydrogenases in the sulfate-reducing bacterium *Desulfovibrio vulgaris* Hildenborough, J. Bacteriol. 189 (2007) 6159–6167.

[51] J.W. Peters, G.J. Schut, E.S. Boyd, D.W. Mulder, E.M. Shepard, J.B. Broderick, P. W. King, M.W.W. Adams, [FeFe]- and [NiFe]-hydrogenase diversity, mechanism, and maturation, Biochimica et Biophysica Acta (BBA) - Molecular, Cell Res. 1853 (2015) 1350–1369.

[52] S. Azabou, T. Mechichi, B.K.C. Patel, S. Sayadi, Isolation and characterization of a mesophilic heavy-metals-tolerant sulfate-reducing bacterium *Desulfomicrobium sp.* from an enrichment culture using phosphogypsum as a sulfate source, J. Hazard. Mater. 140 (2007) 264–270.

[53] M. Martins, M.L. Faleiro, R.J. Barros, A.R. Verissimo, M.A. Barreiros, M.C. Costa, Characterization and activity studies of highly heavy metal resistant sulphate-reducing bacteria to be used in acid mine drainage decontamination, J. Hazard. Mater. 166 (2009) 706–713.

[54] G. Cabrera, R. Pérez, J.M. Gómez, A. Ábalos, D. Cantero, Toxic effects of dissolved heavy metals on *Desulfovibrio vulgaris* and *Desulfovibrio sp.* strains, J. Hazard. Mater. 135 (2006) 40–46.

[55] Y.V. Nancharaiah, S.V. Mohan, P.N. Lens, Biological and bioelectrochemical recovery of critical and scarce metals, Trends Biotechnol. 34 (2016) 137–155.
[56] D.C. Gillan, Metal resistance systems in cultivated bacteria: Are they found in complex communities, Curr. Opin. Biotechnol. 38 (2016) 123–130.
[57] M. Koschorreck, W. Geller, T. Neu, S. Kleinsteuber, T. Kunze, A. Trosiener, K. Wendt-Potthoff, Structure and function of the microbial community in an in situ reactor to treat an acidic mine pit lake, FEMS Microbiol. Ecol. 73 (2010) 385–395.